Bull. Environ. Contam. Toxicol. (1995) 54:479–487

Environmental Contamination and Toxicology

Calculated Three Dimensional Structures of the Fumonisin B_{1-4} Mycotoxins

R. C. Beier, M. H. Elissalde, L. H. Stanker

Food Animal Protection Research Laboratory, Agricultural Research Service, U.S. Department of Agriculture, 2881 F & B Road, College Station, Texas 77845-9594, USA

Received: 3 September 1994/Accepted: 1 December 1994

Fusarium moniliforme Sheldon is one of the most important ear rot pathogens of maize (*Zea mays* L.) and other grains throughout the world (Booth 1971). When fed to horses, corn infected with *F. moniliforme* produced clinical signs and lesions typical of the fatal neurotoxic syndrome, equine leukoencephalomalacia (ELEM) (Wilson and Maronpot 1971; Wilson *et al.* 1973). ELEM of horses and other equines is characterized by liquefaction necrosis of the white matter of one or both cerebral hemispheres (Wilson *et al.* 1985). ELEM is a disease reported in the U.S. since the early 1900's and known in Egypt, Africa, China, Japan, and European countries (Buck *et al.* 1979; Haliburton and Buck 1986; Marasas *et al.* 1988; McCue 1989). Corn samples associated with ELEM caused hepatotoxicity and renal toxicity in male Sprague-Dawley rats (Voss *et al.* 1989). *F. moniliforme* cultures caused porcine pulmonary edema (PPE) (Kriek *et al.* 1981; Ross *et al.* 1990), acute nephrosis and hepatosis in sheep, and cirrhosis, intraventricular cardiac thrombosis, and nephrosis in rats (Kriek *et al.* 1981), and were shown to have cancer-promoting activity (Gelderblom *et al.* 1988).

Four biologically active fumonisins have been isolated and characterized. Fumonisins B_1 and B_2 (FB_1 and FB_2) (Fig. 1) (Bezuidenhout *et al.* 1988), and fumonisins B_3 and B_4 (FB_3 and FB_4) (Fig. 1) (Gelderblom *et al.* 1992; Plattner *et al.* 1992) were isolated from the culture material of *F. moniliforme*. The first experimental evidence that FB_1 caused ELEM was presented by Marasas *et al.* (1988). Horses orally dosed with FB_1 developed ELEM (Kellerman *et al.* 1990), and ponies developed ELEM, hepatic necrosis, and encephalopathy (Ross *et al.* 1993).

In swine, PPE syndrome can be caused by IV injection of FB_1 (Harrison *et al.* 1990). From a series of studies with pigs, either PPE or liver failure emerged as

Mention of a trade name, proprietary product, or specific equipment does not constitute a guarantee or warranty by the U.S. Department of Agriculture and does not imply its approval to the exclusion of other products that may be suitable.

Correspondence to: R. C. Beier

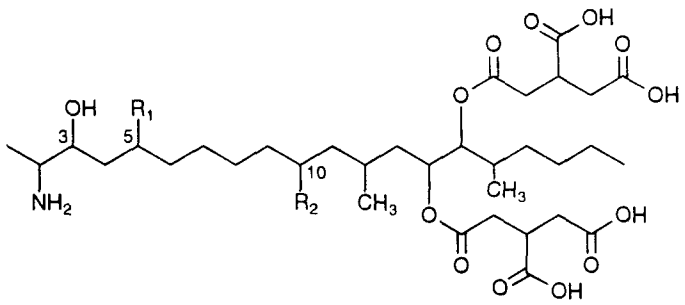

Fumonisin B_1: $R_1 = OH$, $R_2 = OH$
Fumonisin B_2: $R_1 = OH$, $R_2 = H$
Fumonisin B_3: $R_1 = H$, $R_2 = OH$
Fumonisin B_4: $R_1 = H$, $R_2 = H$

Figure 1. Chemical structures of the fumonisins calculated in this study.

distinct pathogenetic expressions of FB_1 toxicoses (Colvin *et al.* 1993). However, young female pigs fed a diet containing FB_1 developed nodular hyperplasia of the liver, and hyperplastic plaques within the distal esophageal mucosa (Casteel *et al.* 1993). It was shown that FB_1 undergoes enterohepatic cycling in the pig, and has affinity for specific tissues, particularly the liver (Prelusky *et al.* 1994).

Male and female rats fed diets fortified with FB_1 caused hepatotoxicity and cortical nephrosis in both sexes (Voss *et al.* 1993). Both the hepatic and renal lesions were consistent with those found in rats consuming *F. moniliforme*-infected corn (Voss *et al.* 1989; Plattner *et al.* 1990). Purified FB_1 is capable of inducing the subchronic liver and kidney lesions attributed to *F. moniliforme* cultures (Voss *et al.* 1993). FB_1 caused prenatal deaths and resorptions in hamsters (Floss *et al.* 1994). Turkey poults treated with FB_1 developed biliary hyperplasia, hypertrophy of Kupffer's cells, and thymic cortical atrophy (Weibking *et al.* 1993).

An isolate of *F. moniliforme*, strain MRC 826, was obtained from corn collected in Transkei, Union of South Africa, where the human esophageal cancer rate is high (Marasas *et al.* 1979). MRC 826 was found to be mutagenic (Gelderblom *et al.* 1983). The main fumonisin produced by *F. moniliforme*, FB_1, was shown to have cancer-promoting activity similar to the fungal culture material (Gelderblom *et al.* 1988). A mammalian cell line of MDCK dog kidney epithelial cells was sensitive to FB_1 and FB_2 (Fig. 1) (Shier *et al.* 1991). FB_2 inhibited renal epithelial cell (LLC-PK) proliferation resulting in cell death (Yoo *et al.* 1992).

Biochemical findings show that FB_1 and FB_2 are the first naturally occurring inhibitors of sphingosine and sphinganine *N*-acyltransferase in rat primary hepatocytes (Wang *et al.* 1991). Fumonisins inhibit the conversion of sphinganine to *N*-acyl-sphinganines. It was suggested that the disruption of the *de novo* pathway of sphingolipid biosynthesis may be a critical event in the diseases associated with fumonisin consumption (Wang *et al.* 1991).

The fumonisins are a good example of a naturally occurring world wide environmental contamination caused by a fungus. FB_{1-3} are the major naturally produced fumonisins from *F. moniliforme*, and FB_4 is produced in only minor quantities (Cawood *et al.* 1991). FB_1 is the most abundant member of the fumonisin family and usually accounts for about 70% of the total fumonisins (Plattner *et al.* 1992). As seen above, there are a large number of effects observed in animals and humans caused by FB_1. There may be multiple effects in any one species, and the effects generally vary from specie to specie. However, there is only one known biochemical action of FB_1 and FB_2; the inhibition of sphingolipid biosynthesis.

The purpose of this study is to determine the lowest energy 3-dimensional conformations available to FB_{1-4} through molecular modeling methods. These structures may produce additional insight into other potential activities that may be associated with these molecules.

MATERIALS AND METHODS

Molecular modeling studies were performed using a CAChe™ WorkSystem with release 3.5 software running on a Macintosh Quadra 700 equipped with a RP88 coprocessor board and a CAChe™ stereoscopic display (CAChe™ Scientific, Inc., Beaverton, OR). Minimum potential energy conformations of all compounds shown in Fig. 2 and 3 were calculated using molecular mechanics with Allinger's standard MM2 force field parameters (Allinger 1977) augmented to contain force field parameters for cases not addressed by MM2 (CAChe™ Scientific, Inc.). A good description of molecular mechanics and its underlying philosophy is presented by Boyd and Lipkowitz (1982). Molecular mechanics calculations utilized the conjugate gradient optimization technique. Following the initial geometrical optimization, a one pass sequential search to determine the lowest potential energy conformations was performed by rotating all dihedral angles through 360° in 15° increments. Following the initial sequential search, multiple multipass sequential searches of four dihedral angles through 360° in 15° increments at a time were conducted to determine the lowest potential energy for the interacting systems of atoms. One final multipass sequential search of each set of dihedral angles through 90° or 180° in 5° to 7.5° increments was conducted for refinement of the optimum geometries. At completion of each sequential search a geometrical optimization was performed on each of the 5 to 10 selected structures

having the lowest potential energies. The resultant lowest potential energy structure was then used for the next refinement calculation. The set of structures resulting from each sequential calculation were viewed using the CAChe™ Visualizer+ graphics application.

To obtain the electron density distribution of FB_1, the final structure of FB_1 as obtained from molecular mechanics calculations was then re-calculated using ExtHückel to obtain all of the molecular orbitals. The resultant file was submitted to the tabulator to convert the results of the computational methods into 3D coordinates required by the CAChe Visualizer+ application. The final results showing the electron density of FB_1 was observed using the Visualizer+ application.

Stereo ball and cylinder representations were copied to the clipboard in the print preview mode. These figures were pasted into McDraw II for sizing and attaching coding on the spheres to represent the atom type. The ball and cylinder models were printed on a Macintosh Personal LaserWriter at 300 dots/inch and the electron density models were printed on a Macintosh LaserWriter Select 360 at 600 dots/inch using the following Macintosh print settings: high-quality shaded, color/gray scale, high resolution and faster postscript printing mode.

RESULTS AND DISCUSSION

The molecular mechanics calculated structures for FB_1 and FB_2 (Fig. 2), and FB_3 and FB_4 (Fig. 3) are represented as ball and cylinder stereo models. Carbon atoms are depicted as black spheres, hydrogen atoms are open spheres, nitrogen atoms are cross-hatched spheres, and oxygen atoms are represented as spheres with vertical lines. The use of a stereoscope gives each set of molecules a three dimensional appearance. The four molecules each have a unique folded structure that one might liken to that of a folded peptide. FB_1 has more internal hydrogen bonding with the hydroxyl moiety at both C-5 and C-10 than does FB_2 or FB_3 which have only one hydroxyl at C-5 and C-10, respectively. FB_4 has the least potential internal hydrogen bonding with no hydroxyls at either the C-5 or C-10 positions.

A very interesting cage-like structure is formed by the folding of the amine back bone with the two esterified trimethylpropane-1,2,3-tricarboxylic acid side chains. The loss of a hydroxyl at C-5 or C-10 in FB_2 and FB_3, respectively, allows this cage to become smaller than predicted for FB_1. The three dimensional structure formed is similar to the claw of a bird. Recently, the observance of the fumonisins folding into this cage through molecular modeling has allowed the postulation of why the monoclonal antibodies produced to FB_1 linked through the amino group have lower specificities for free FB_1 than expected (Elissalde *et al.* 1995). This cage-like structure brings the amine, hydroxyls, and carboxylic acid groups into

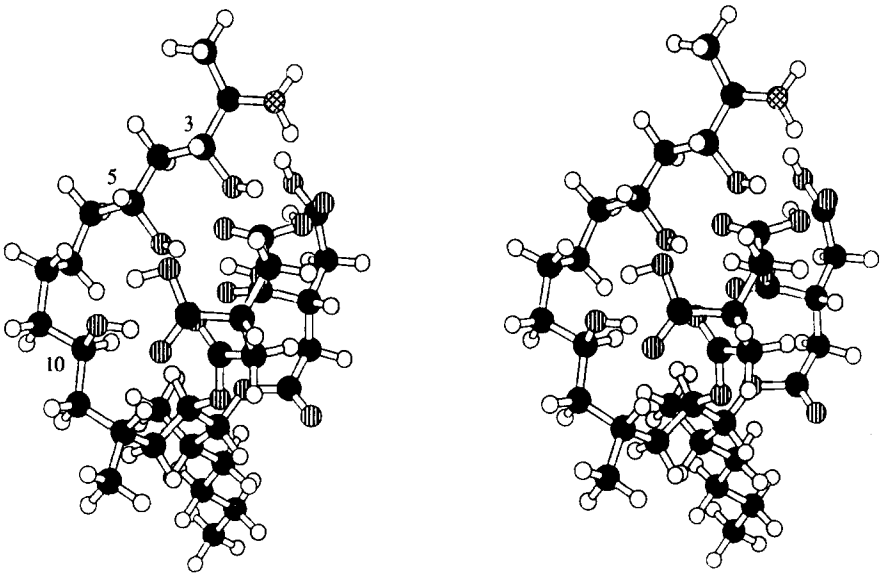

Fumonisin B_1

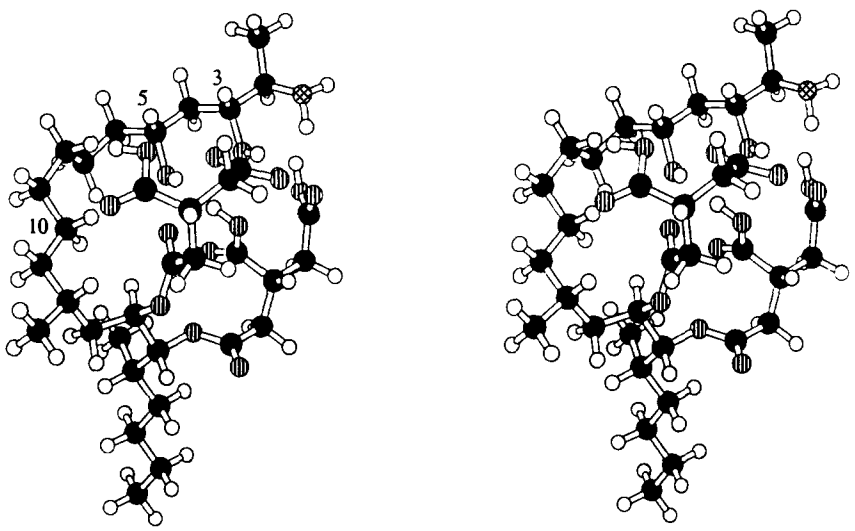

Fumonisin B_2

Figure 2. Ball and cylinder stereo-models of the minimum energy conformations of fumonisins B_1 and B_2. Carbon atoms are depicted as black spheres, hydrogen atoms are open spheres, nitrogen atoms are cross-hatched spheres, and oxygen atoms are represented as spheres with vertical lines.

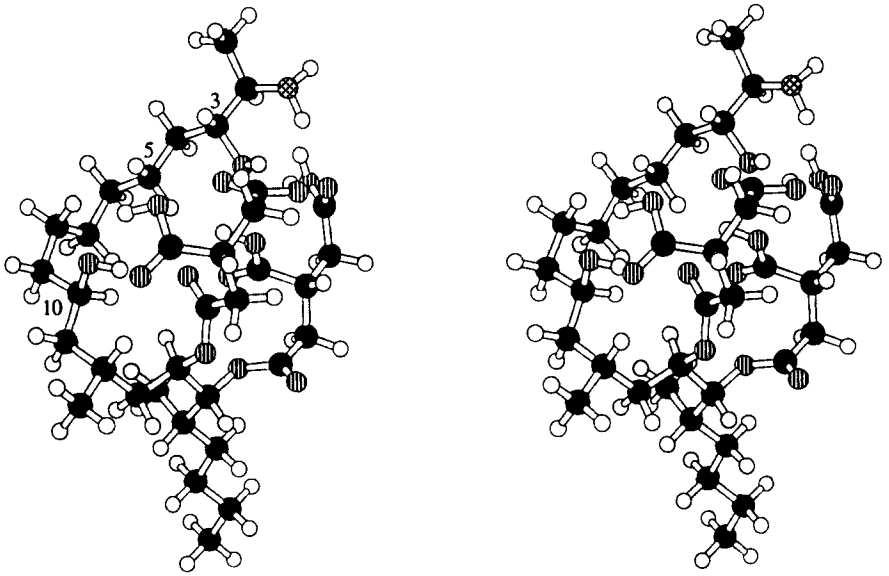

Fumonisin B_3

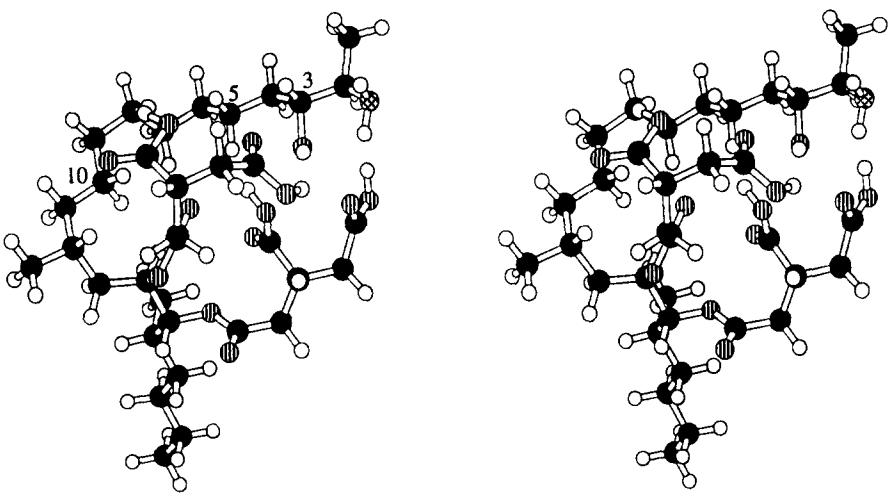

Fumonisin B_4

Figure 3. Ball and cylinder stereo-models of the minimum energy conformations of fumonisins B_3 and B_4. Carbon atoms are depicted as black spheres, hydrogen atoms are open spheres, nitrogen atoms are cross hatched spheres, and oxygen atoms are represented as spheres with vertical lines.

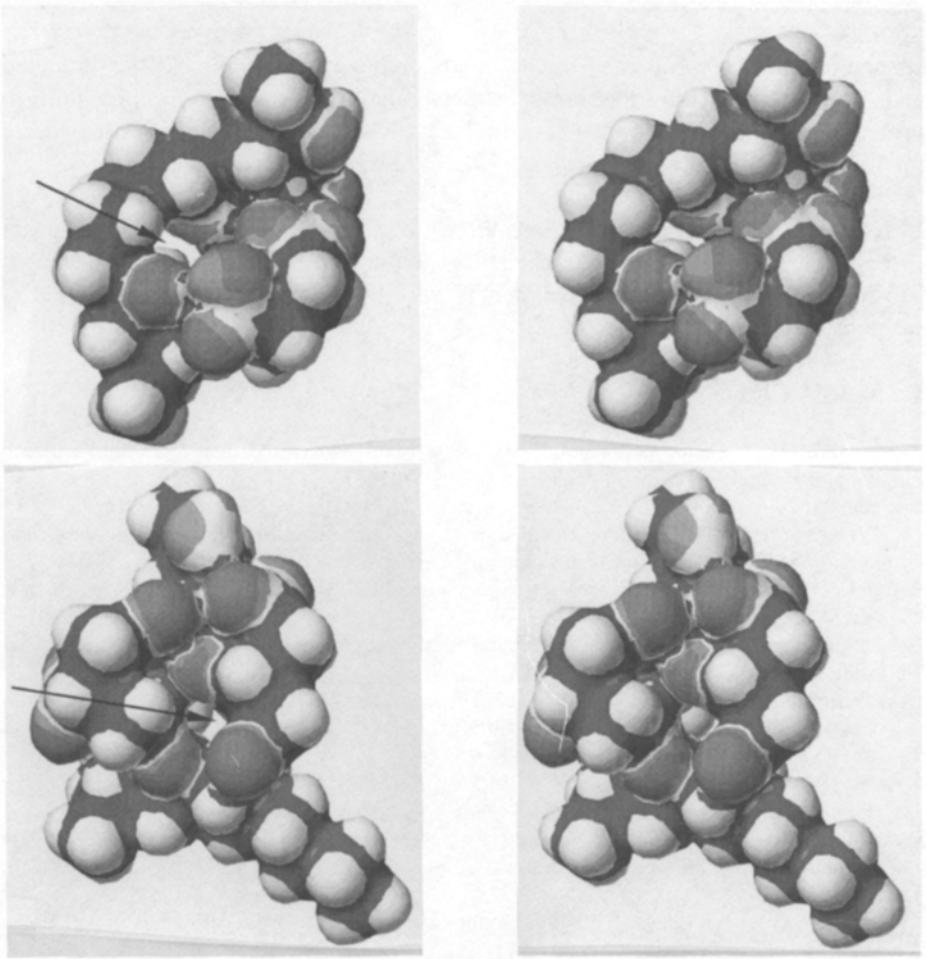

Figure 4. Left and right stereo views of the electron density distribution for FB_1 looking at the electrophilic end (top view) and lipophilic end (bottom view). The arrows show spaces within FB_1 that traverse from the electrophilic to the lipophilic part of the molecule.

close proximity. Both the structures of these molecules and the close association of the amine, carboxylic acid groups, and hydroxyls suggests that these molecules may have chelator-type activity.

Fig. 4 shows two stereo views of the electron density distribution for FB_1. The use of a stereoscope gives each set of stereo views a three dimensional appearance. The top view shows the electrophilic end of the molecule and the bottom view is a side presentation that shows the lipophilic end. In both views, arrows point out large channels within the center of FB_1 that have no electron density. This space or hole begins on the electrophilic end and transverses the molecule, bifurcating, and opening in two locations to either side of the lipophilic end. These spaces may

change in size as a result of changing hydrogen bonding patterns. If the lipophilic end of FB_1 were imbedded into a membrane with the electrophilic portion protruding; the membrane may become leaky due to these spaces or holes within the fumonisin structure.

Based upon structural interpretations after molecular modeling of FB_1, it appears that these molecules may act as chelators, or they may cause membrane leakage. This hypothesis will require experimental work for corroboration of the structure reactivity relationship.

REFERENCES

Allinger NL (1977) Conformational analysis. 130. MM2. A hydrocarbon force field utilizing V_1 and V_2 torsional terms. J Am Chem Soc 99:8127–8134.

Bezuidenhout SC, Gelderblom WCA, Gorst-Allman CP, Horak RM, Marasas WFO, Spiteller G, Vleggaar R (1988) Structure elucidation of the fumonisins, mycotoxins from *Fusarium moniliforme*. J Chem Soc Chem Commun 743–745.

Booth C (1971) The Genus *Fusarium*. Commonwealth Mycological Institute, Kew, Surrey, England.

Boyd DB, Lipkowitz KB (1982) Molecular mechanics: The method and its underlying philosophy. J Chem Educ 59:269–274.

Buck WB, Haliburton JC, Thilsted JP, Lock TF, Vesonder RF (1979) Equine leukoencephalomalacia: Comparative pathology of naturally occurring and experimental cases. Proc Ann Meet - Am Assoc Vet Lab Diagn 22:239–258.

Casteel SW, Turk JR, Cowart RP, Rottinghaus GE (1993) Chronic toxicity of fumonisin in weanling pigs. J Vet Diagn Invest 5:413–417.

Cawood ME, Gelderblom WCA, Vleggaar R, Behrend Y, Thiel PG, Marasas WFO (1991) Isolation of the fumonisin mycotoxins: A quantitative approach. J Agric Food Chem 39:1958–1962.

Colvin BM, Cooley AJ, Beaver RW (1993) Fumonisin toxicosis in swine: clinical and pathologic findings. J Vet Diagn Invest 5:232–241.

Elissalde MH, Kamps-Holtzapple C, Beier RC, Plattner RD, Rowe LD, Stanker LH (1995) Molecular modeling of fumonisin B_{1-3} and development of a monoclonal-based enzyme linked immunosorbent assay for these mycotoxins. Food Agric Immunol (In Press).

Floss JL, Casteel SW, Johnson GC, Rottinghaus GE, Krause GF (1994) Developmental toxicity in hamsters of an aqueous extract of *Fusarium moniliforme* culture material containing known quantities of fumonisin B_1. Vet Hum Toxicol 36:5–10.

Gelderblom WCA, Jaskiewicz K, Marasas WFO, Thiel PG, Horak RM, Vleggaar R, Kriek NPJ (1988) Fumonisins—Novel mycotoxins with cancer-promoting activity produced by *Fusarium moniliforme*. Appl Environ Microbiol 54:1806–1811.

Gelderblom WCA, Marasas WFO, Vleggaar R, Thiel PG, Cawood ME (1992) Fumonisins: Isolation, chemical characterization and biological effects. Mycopathologia 117:11–16.

Gelderblom WCA, Thiel PG, van der Merwe KJ, Marasas WFO, Spies HSC (1983) A mutagen produced by *Fusarium moniliforme*. Toxicon 21:467–473.

Haliburton JC, Buck WB (1986) Equine leukoencephalomalacia. Curr Top Vet Med Anim Sci 33:75–79.

Harrison LR, Colvin BM, Greene JT, Newman LE, Cole JR (1990) Pulmonary edema and hydrothorax in swine produced by fumonisin B_1, a toxic metabolite of *Fusarium moniliforme*. J Vet Diagn Invest 2:210–212.

Kellerman TS, Marasas WFO, Thiel PG, Gelderblom WCA, Cawood M, Coetzer JAW (1990) Leukoencephalomalacia in two horses induced by oral dosing of fumonisin B_1. Onderstepoort J Vet Res 57:269–275.

Kriek NPJ, Kellerman TS, Marasas WFO (1981) A comparative study of the toxicity of *Fusarium verticillioides* (= *F. moniliforme*) to horses, primates, pigs, sheep, and rats. Onderstepoort J Vet Res 48:129–131.

Marasas WFO, Kellerman TS, Gelderblom WCA, Coetzer JAW, Thiel PG, van der Lugt JJ (1988) Leukoencephalomalacia in a horse induced by fumonisin B_1 isolated from *Fusarium moniliforme*. Onderstepoort J Vet Res 55:197–203.

Marasas WFO, van Rensburg SF, Mirocha SJ (1979) Incidence of *Fusarium* species and the mycotoxins, deoxynivalenol and zearalenone, in corn produced in esophageal cancer areas in Transkei. J Agric Food Chem 27:1108–1112.

McCue PM (1989) Equine leukoencephalomalacia. Compendium 11:646–651.

Plattner RD, Norred WP, Bacon CW, Voss KA, Peterson R, Shackelford DD, Weisleder D (1990) A method of detection of fumonisins in corn samples associated with field cases of equine leukoencephalomalacia. Mycologia 82:698–702.

Plattner RD, Weisleder D, Shackelford DD, Peterson R, Powell RG (1992) A new fumonisin from solid cultures of *Fusarium moniliforme*. Mycopathologia 117:23–28.

Prelusky DB, Trenholm HL, Savard ME (1994) Pharmacokinetic fate of ^{14}C-labelled fumonisin B_1 in swine. Natl Toxins 2:73–80.

Ross PF, Ledet AE, Owens DL, Rice LG, Nelson HA, Osweiler GD, Wilson TM (1993) Experimental equine leukoencephalomalacia, toxic hepatosis, and encephalopathy caused by corn naturally contaminated with fumonisins. J Vet Diagn Invest 5:69–74.

Ross PF, Nelson PE, Richard JL, Osweiler GD, Rice LG, Plattner RD, Wilson TM (1990) Production of fumonisins by *Fusarium moniliforme* and *Fusarium proliferatum* isolates associated with equine leukoencephalomalacia and a pulmonary edema syndrome in swine. Appl Environ Microbiol 56:3225–3226.

Shier WT, Abbas HK, Mirocha CJ (1991) Toxicity of the mycotoxins fumonisins B_1 and B_2 and *Alternaria alternata* f. sp. *lycopersici* toxin (AAL) in cultured mammalian cells. Mycopathologia 116:97–104.

Voss KA, Chamberlain WJ, Bacon CW, Norred WP (1993) A preliminary investigation on renal and hepatic toxicity in rats fed purified fumonisin B_1. Natl Toxins 1:222–228.

Voss KA, Norred WP, Plattner RD, Bacon CW (1989) Hepatotoxicity and renal toxicity in rats of corn samples associated with field cases of equine leukoencephalomalacia. Food Chem Toxicol 27:89–96.

Wang E, Norred WP, Bacon CW, Riley RT, Merrill AH Jr (1991) Inhibition of sphingolipid biosynthesis by fumonisins. J Biol Chem 266:14486–14490.

Weibking TS, Ledoux DR, Brown TP, Rottinghaus GE (1993) Fumonisin toxicity in turkey poults. J Vet Diagn Invest 5:75–83.

Wilson BJ, Maronpot RR (1971) Causative fungal agent of leucoencephalomalacia in equine animals. Vet Rec 88:484–485.

Wilson BJ, Maronpot RR, Hildebrandt PK (1973) Equine leukoencephalomalacia. J Am Vet Med Assoc 163:1293–1295.

Wilson TM, Nelson PE, Ryan TB, Rouse CD, Pittman CW, Neal TP, Porterfield ML, Saunders GK (1985) Linking leukoencephalomalacia to commercial horse rations. Equine Pract 80:63–69.

Yoo H-S, Norred WP, Wang E, Merrill AH Jr, Riley RT (1992) Fumonisin inhibition of *de Novo* sphingolipid biosynthesis and cytotoxicity are correlated in LLC-PK cells. Toxicol Appl Pharmacol 114:9–15.